Materials Science and Engineering A 552 (2012) 112–118

Contents lists available at SciVerse ScienceDirect

Materials Science and Engineering A

journal homepage: www.elsevier.com/locate/msea

Evaluation of the effect of nitrogen on creep properties of 316LN stainless steel from impression creep tests

Naveena, V.D. Vijayanand, V. Ganesan, K. Laha, M.D. Mathew*

Mechanical Metallurgy Division, Indira Gandhi Centre for Atomic Research, Kalpakkam 603 102, India

ARTICLE INFO

Article history:
Received 19 March 2012
Accepted 8 May 2012
Available online 22 May 2012

Keywords:
Impression creep
316LN stainless steel
Impression velocity
Punching stress
Effect of nitrogen

ABSTRACT

Impression creep testing technique is an innovative tool to study creep deformation behavior of materials mainly because it requires relatively short test time and small volume of material for evaluating the creep properties when compared with conventional uniaxial creep testing which is both material and time consuming. The effect of nitrogen on creep deformation behavior of type 316LN stainless steel has been studied using impression creep testing technique. Impression creep tests have been carried out at 923 K up to 1000 h on 316LN stainless steel containing 0.07, 0.11, 0.14, and 0.22 wt.% nitrogen, in the punching stress range of 400–800 MPa. The impression creep curves were characterized by a loading strain, a primary creep stage, and a secondary creep stage similar to uniaxial creep curves. The tertiary stage observed in uniaxial creep tests was absent. The steady state impression velocity was found to increase with increasing punching stress. The calculated stress exponent values varied between 3.3 and 8.2 with increasing in nitrogen content. It was observed that impression velocity was sensitive to the variation in nitrogen content in the steel. The steady state impression velocity was found to decrease with increasing nitrogen content. Correlation between the impression creep parameters and conventional uniaxial creep parameters has been established based on the laws of mechanics for time dependent plasticity.

1. Introduction

Uniaxial creep testing technique is the most commonly used test method for characterization of creep deformation behavior of materials. The test specimens used for these studies are of standard geometry and require a considerable volume of material for specimen preparation. Further, it requires many such specimens to carryout multiple creep tests at different temperatures and stress levels in order to assess various creep deformation parameters. Hence, the test methodology is both time and material consuming. As a result, in some cases where the amount of material available for testing is small or in the case of rapid screening of several laboratory heats for alloy development, small sized specimen testing techniques are desirable. In view of this, there is considerable interest in developing small specimen testing techniques for evaluation of creep properties. Several attempts have been made earlier to obtain creep properties of materials by using a simple long time indentation hardness test [1–10]. Although some degree of success was achieved in these investigations, the major drawback in this methodology was the continuous decrease in the stress with the time of indentation. This is because of the geometry of the indenter (conical, spherical or pyramidal indenters) which is employed in these tests. During the test, the contact area increases with time of indentation which results in continuous decrease in stress and thus, no steady state is attained. In order to circumvent this problem, impression creep testing technique has been developed. Impression creep test is a modified indentation creep test where conical, pyramidal or spherical indenters are replaced by a flat-ended cylindrical indenter. This technique was first suggested by Chu and Li [11,12]. In this technique, a constant load is applied to a flat-ended cylindrical indenter. Since the cross-sectional area of the indenter remains constant, the constant load applied to the punch implies a constant punching stress. During the test, the displacement of the cylindrical punch is recorded as a function of the elapsed time. Initially, the penetration rate or impression velocity decreases with time and then reaches steady state after a transient period. The impression creep curves are similar to the conventional creep curves, but they exhibit only the first two characteristic stages of the creep curve – the transient and the steady state. There is no tertiary creep stage in impression creep curve. This is because of the fact that in impression creep test, loading is compressive in nature as a consequence necking and fracture of the sample do not occur. The slope of the steady state part of the curve gives the steady state impression velocity. The punch penetration rate or impression velocity is controlled by the time dependence of the movement of the material under the punch and thus directly

* Corresponding author. Tel.: +91 44 27480003; fax: +91 44 27480075.
E-mail address: mathew@igcar.gov.in (M.D. Mathew).

0921-5093/$ – see front matter © 2012 Elsevier B.V. All rights reserved.
http://dx.doi.org/10.1016/j.msea.2012.05.017

Table 1
Chemical composition (in wt.%) of type 316LN stainless steel.

Designation	Chemical composition (in wt.%)									
	N	C	Mn	Cr	Mo	Ni	Si	S	P	Fe
7N	0.07	0.027	1.7	17.53	2.49	12.2	0.22	0.0055	0.013	Bal.
11N	0.11	0.033	1.78	17.62	2.51	12.27	0.21	0.0055	0.015	Bal.
14N	0.14	0.025	1.74	17.57	2.53	12.15	0.2	0.0041	0.017	Bal.
22N	0.22	0.028	1.7	17.57	2.54	12.36	0.2	0.0055	0.018	Bal.

monitors the creep deformation of a localized volume of material [13].

Nitrogen-alloyed low carbon grade type 316LN stainless steel is used as a major structural material for high temperature components in fast breeder reactors. Impression creep is very attractive in the development of new alloys where the rapid screening of material is essential. Tests can be carried out with a minimum volume of material. It is the purpose of the present work to study the effect of variation of nitrogen content on creep deformation behavior of 316LN stainless steel using impression creep testing technique. The study is also aimed at establishing correlation between impression creep parameters and conventional uniaxial creep parameters. Microstructural changes observed in the impression creep tested material have also been discussed in order to understand the deformation mechanism associated with impression creep in the alloys under investigation.

2. Experimental details

2.1. Material and sample preparation

The present investigation involved four heats of 316LN stainless steel containing 0.07, 0.11, 0.14, and 0.22 wt.% nitrogen. The chemical compositions of these alloys are given in Table 1. Rectangular blocks of 12 mm thickness were machined to get the flat surfaces and the impression creep testing surfaces of the specimens were polished to a 1 μm finish using standard metallographic techniques. The final dimension of the specimens used for the impression creep tests were 20 mm × 20 mm × 10 mm. Fig. 1 shows the microstructure of the material before testing which was solution treated at 1373 K for 1 h followed by water quenching. Nearly equiaxed grains with an average grain size of about 85 μm were observed.

2.2. Impression creep testing system

The impression creep testing system used for these studies is shown in Fig. 2. The system consists of specimen cage with two frames – one fixed to the bottom plate of the specimen cage and the other connected to the pull rod which is free to move. The former has an indenter holder to which the indenter is fixed and the latter has a sample holder over which test specimen is placed exactly below the indenter. Indenters are made of tungsten carbide. The pull rod is connected to the lever arm with 1:10 lever ratio. The vertical movement of the pull rod and hence the impression depth is sensed through a Linear Variable Differential Transducer (LVDT) with an accuracy better than ±0.5%. A load cell of maximum capacity 980 N is attached to the load train in order to measure the load accurately. The temperature control system is capable of maintaining the temperature constant with an accuracy of ±1 °C. A vacuum system which can produce a vacuum level up to 10^{-6} mbar is used to avoid oxidation of the specimen at higher test temperatures. Data is recorded using a PC based online data acquisition system.

2.3. Impression creep experiments and microstructural evaluation

Impression creep tests were conducted at 923 K on 316LN stainless steel containing 0.07, 0.11, 0.14, and 0.22 wt.% nitrogen under four different punching stress levels of 472, 591, 675, and 760 MPa. A cylindrical punch of 1 mm diameter was employed for this study. The experiments were carried out in vacuum (10^{-6} mbar) in order to avoid the oxidation of the specimens.

In order to characterize the microstructural changes associated with the creep deformation in the tested material, the impression creep tested specimen was sectioned along the diameter of the impression direction in the middle of the impressed area. The sectioned surface was polished to 1 μm finish using standard metallographic techniques. The polished sample was etched electrolytically with 60% nitric acid in water (60 ml HNO_3 + 40 ml H_2O). Microstructural evolution was investigated using optical and scanning electron microscope (SEM).

3. Analysis of impression creep parameters

3.1. Evaluation of punching stress and impression velocity

In impression creep test, a constant load L is applied to the test specimen through a cylindrical punch of diameter d. The mean pressure under the punch is referred to as the punching stress and is given by,

$$\sigma_{imp} = \frac{4L}{\pi d^2} \quad (1)$$

Under the punching stress σ_{imp}, the cylindrical punch penetrates into the surface of the test specimen to a depth h in time t. The rate at which the cylindrical punch penetrates the specimen surface is referred to as impression velocity and is given by,

$$v_{imp} = \frac{dh}{dt} \quad (2)$$

3.2. Equivalence between impression creep parameters and conventional uniaxial creep parameters

For the characterization of creep behavior of materials using impression creep test, it is essential to establish correlations between the impression creep parameters (σ_{imp}, v_{imp}) and uniaxial creep parameters (σ_{uni}, $\dot{\varepsilon}_{uni}$). The steady state strain rate $\dot{\varepsilon}_{uni}$ in uniaxial creep test correlates with the ratio of impression velocity v_{imp} to the punch diameter d used in the impression creep test. Empirically, there is a factor, about 0.33, which converts the punching stress σ_{imp} to an equivalent stress σ_{uni} in conventional uniaxial creep tests. These relations have been established numerically by finite element calculations [14] and verified experimentally [11,12,15].

It is generally accepted that for materials obeying power-law creep, the steady state strain rate $\dot{\varepsilon}_{uni}$ is related to the uniaxial stress σ_{uni} by,

$$\dot{\varepsilon}_{uni} = A\sigma_{uni}^{n} \quad (3)$$

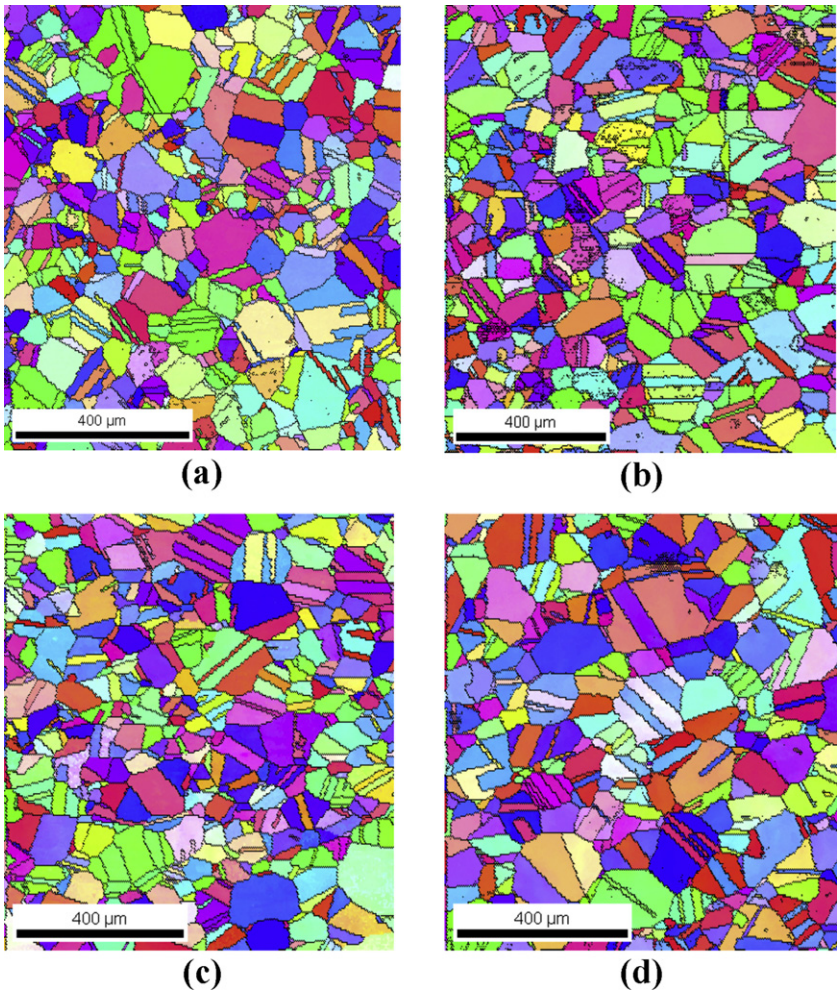

Fig. 1. Microstructure of solution annealed 316LN stainless steel containing: (a) 0.07, (b) 0.11, (c) 0.14, and (d) 0.22 wt.% nitrogen.

where n is the stress exponent and A is the power law coefficient which incorporates the temperature dependence of steady state strain rate. Li and co-workers [11,14,16] carried out finite element analysis for materials obeying power-law creep. The impression creep experiment was simulated by considering power law constitutive equation for the deformation of each finite element. This power law was between the creep rate and the Von Mises stress. The Von Mises flow rule was used to calculate the various strain components. The calculation was done for many time intervals until a trend toward a steady state was clearly indicated. It was found that the impression velocity v_{imp} was proportional to the punch diameter and had the same stress dependence as was observed in the conventional uniaxial creep test. Hence,

$$\frac{v_{imp}}{d} \propto \sigma_{imp}^{n} \tag{4}$$

where, v_{imp} is the impression velocity, σ_{imp} is the punching stress, d is the diameter of the punch and n is the stress exponent value.

Researchers have generally resorted to trial-and-error method to correlate σ_{imp} and v_{imp}/d in impression creep to σ_{uni} and $\dot{\varepsilon}_{uni}$ in conventional uniaxial creep. The general forms of these correlations are,

$$\sigma_{uni} = \alpha\sigma_{imp} \tag{5}$$

and,

$$\dot{\varepsilon}_{uni} = \frac{v_{imp}}{\beta d} \tag{6}$$

where, α and β are the correlation factors.

Experimentally determined values of α range from 0.26 to 0.36 for a range of materials such as Pb, TiAl alloys, Mg–8Zn–4Al–0.5Ca alloy, Zn, cast Mg–5Sn–xCa alloys, 316 stainless steel [11,15,17–21]. Eq. (6) is often used with $\beta = 1$ [11,12,17,18,20]. For the present analysis, we used the conversion factors $\alpha = 0.33$ and $\beta = 1$, determined by finite element calculation reported by Yu and Li [14] to relate the creep data from impression and conventional tensile creep tests.

4. Results and discussion

4.1. Impression creep curves

Typical impression creep curves are presented as variation of punch penetration depth with dwell time under different punching stress levels in Figs. 3–6 for 316LN stainless steel containing different nitrogen contents. The creep curves were characterized by a loading strain, a primary creep stage, and a secondary creep stage. However, the tertiary stage that appears in conventional creep curves was found to be absent here. This is attributed to the fact that in impression creep test, loading is compressive in nature; necking and fracture of the sample do not occur. An advantage with the absence of tertiary creep stage is that the deformation of the material under the punch is stable and hence the secondary creep stage sustains for a long time resulting in a true steady state. The longest test time in the investigation was 1000 h.

Fig. 2. Impression creep testing machine.

4.2. Effect of punching stress on impression velocity

The slope of steady state portion of impression creep curve which is referred to as steady state impression velocity was calculated for each stress level. Fig. 7(a) shows the variation of steady state impression velocity with punching stress (log–log plot) for all the four heats. It can be seen that increasing stress at a constant temperature results in higher penetration rates. Steady state impression velocity was found to increase with increasing punching stress. A power law relationship between steady state impression velocity and punching stress was found to be obeyed in all the four heats. The power law exponent (n) varied between

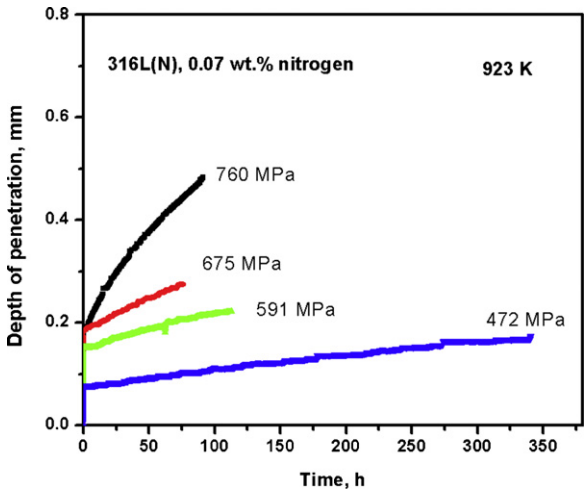

Fig. 3. Plot of impression depth versus time for 316LN stainless steel containing 0.07 wt.% nitrogen at various stress levels.

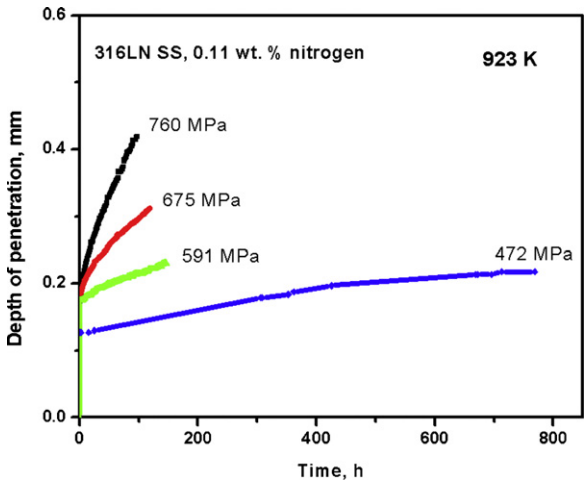

Fig. 4. Plot of impression depth versus time for 316LN stainless steel containing 0.11 wt.% nitrogen at various stress levels.

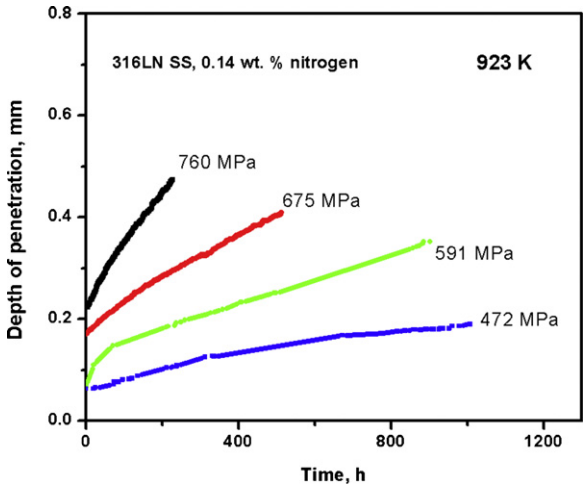

Fig. 5. Plot of impression depth versus time for 316LN stainless steel containing 0.14 wt.% nitrogen at various stress levels.

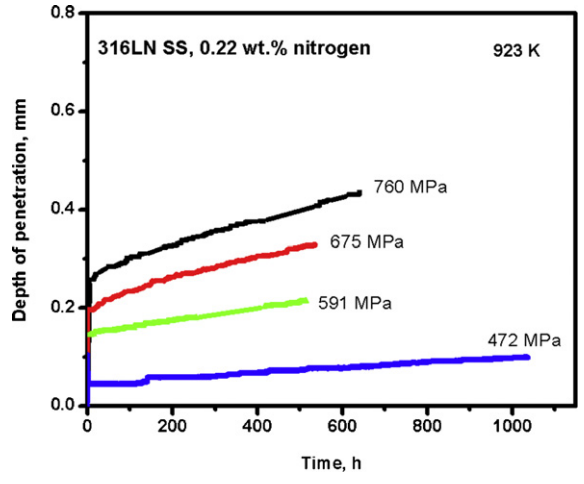

Fig. 6. Plot of impression depth versus time for 316LN stainless steel containing 0.22 wt.% nitrogen at various stress levels.

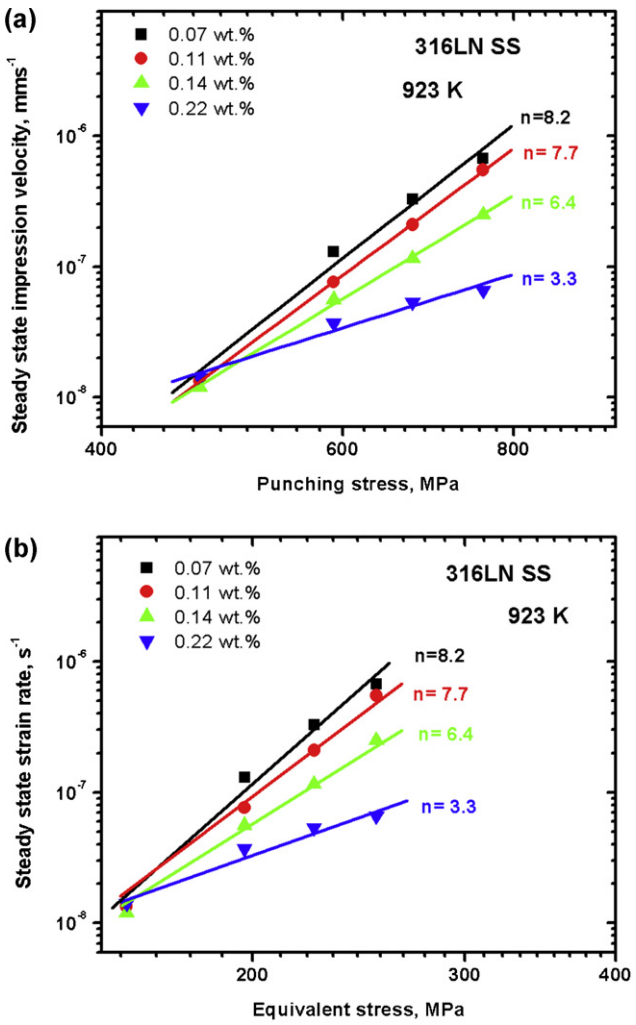

Fig. 7. (a) Variation of steady state impression velocity with punching stress for different nitrogen content. (b) Plot of equivalent steady state strain rates and uniaxial tensile stresses derived from steady state impression velocities and punching stresses using Eqs. (5) and (6) for various nitrogen levels.

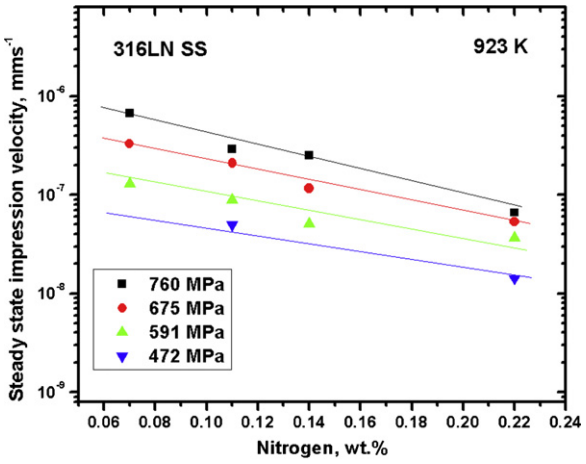

Fig. 8. Variation of steady state impression velocity with nitrogen content in 316LN stainless steel for various stress levels.

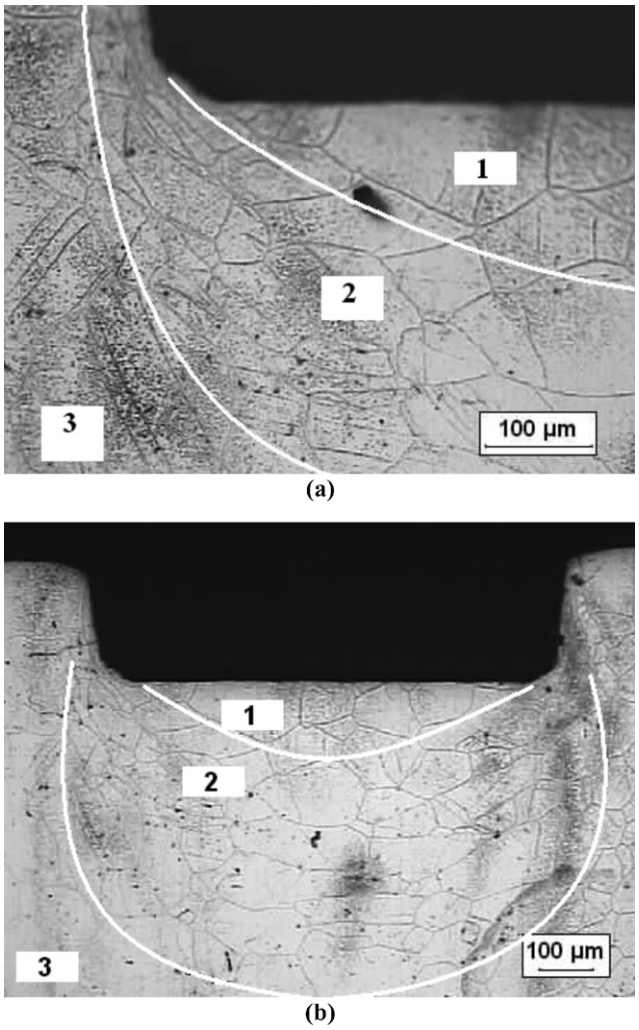

Fig. 9. (a and b) Optical micrographs showing the deformation in the impression creep tested specimen.

3.3 and 8.2 depending upon the nitrogen content in the heat. Similar observations were found in the case of conventional uniaxial creep tests carried out on these materials [22]. Fig. 7(b) shows the plot of equivalent steady state strain rates and uniaxial tensile stresses derived from steady state impression velocities and punching stresses using Eqs. (5) and (6) for various nitrogen levels.

4.3. Influence of nitrogen content on impression velocity

Fig. 8 shows the variation of steady state impression velocity with nitrogen content for different punching stress levels. Impression creep testing technique was found to be sensitive to the variation in creep rate due to very small change in nitrogen content. It was observed that the steady state impression velocity decreased with increasing nitrogen content at all the four stress levels. This result is in good agreement with the results obtained from conventional uniaxial creep tests which showed a decrease in steady state creep rate with increasing nitrogen content [22,23]. Nitrogen was found to be beneficial to creep properties at all the stress levels. Nitrogen is considered to be a potent interstitial solid solution strengthener which improves tensile, creep, and fatigue strength of austenitic stainless steels [24]. Interstitially dissolved nitrogen increases the yield strength and ultimate tensile strength of austenitic stainless steels. The variation of the yield strength with nitrogen content in austenitic stainless steel was reported to

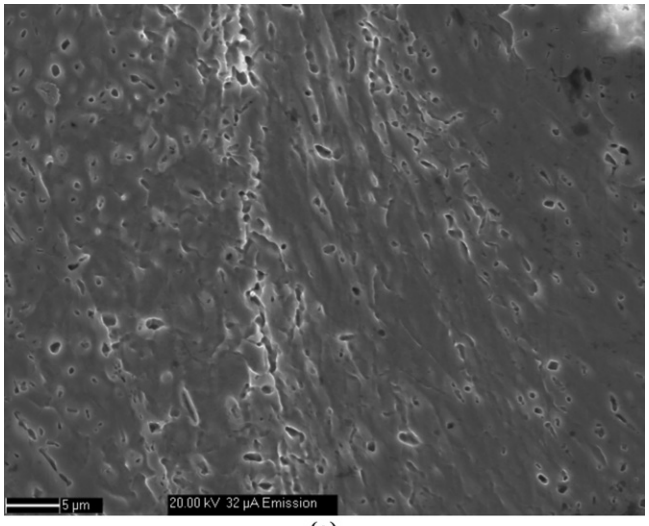

(a)

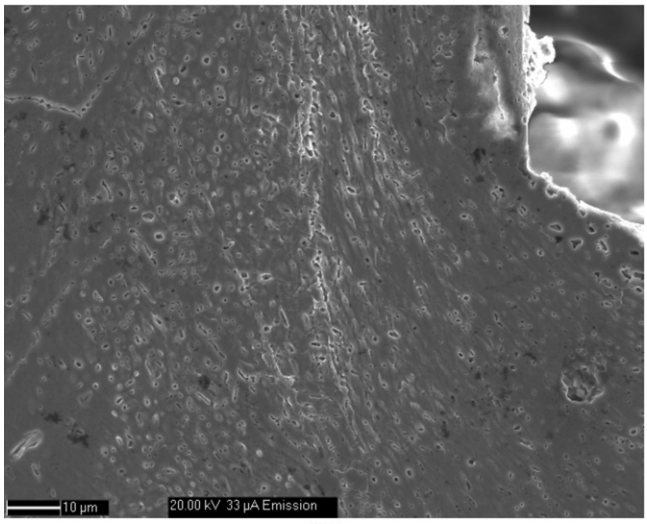

(b)

Fig. 10. (a and b) SEM micrographs showing the material flow pattern near the edge of the indentation in 316LN stainless steel containing 0.14 wt.% nitrogen after the impression creep test.

be linear at room temperature and above [25,26]. The beneficial effect of nitrogen can be attributed to the fact that dissolved nitrogen caused a strong pinning with dislocations [22].

4.4. Microstructural observation in impression creep tested specimen

The microstructural changes observed in the vicinity of the impression in 316LN stainless steel containing 0.14 wt.% nitrogen after the impression creep test is depicted in Fig. 9(a) and (b). Three distinct regions were observed which are labeled with number 1, 2, and 3. In order to distinguish these three distinct regions clearly, curved lines are drawn. In region 1 no significant changes in grain shape were observed. This shows that the stress in this region may be hydrostatic in nature. The material in region 2 was found to experience an extensive shear deformation. For clear observation of the flow pattern in this region, SEM micrographs taken at higher magnification are illustrated in Fig. 10(a) and (b). These line patterns are associated with the material flow during the indentation. The density of these lines is found to be higher near the edge of the indenter than in front of the indenter which indicates that the strain is higher near the edge of the indenter. No change in shape of grains in the region 3 which is far away from the indentation indicates absence of plastic deformation in this region. This clearly demonstrates the localized nature of impression creep test.

5. Conclusions

The effect of nitrogen on the creep deformation behavior of type 316LN stainless steel was investigated by employing the impression creep technique as a faster and non-invasive method and results were correlated with the conventional uniaxial creep test results on the same material. The following conclusions are made based on the investigation carried out.

i) The impression creep curves, presented as the variation of punch penetration depth with dwell time, were found to be similar to the creep curves obtained from conventional uniaxial creep tests. The impression creep curves were characterized by a loading strain, primary, and secondary stages. However, the tertiary stage that appears in conventional creep curves was absent here.
ii) The steady state impression velocity was found to increase with increasing applied stress. A power law relationship was found to obey between the steady state impression velocity and the punching stress in all the four heats.
iii) Impression creep testing technique was found to be sensitive to the variation in creep rate due to change in composition. The steady state impression velocity was found to decrease with increase in nitrogen content. This result was found to be in good agreement with the results obtained from conventional uniaxial creep tests.
iv) A good correspondence between the impression creep test and the conventional creep test results on engineering alloys demonstrates that impression creep could be used to characterize the creep behavior of materials. This is very attractive in alloy development where the material available for testing is small and a rapid screening of several heats are essential.

Acknowledgments

The authors gratefully acknowledge the support and encouragement received from Dr. A.K. Badhuri, Associate Director, Materials Development and Technology group and Dr. T. Jayakumar, Director, Metallurgy and Materials Group, Indira Gandhi Centre for Atomic Research.

References

[1] P.M. Sargent, M.F. Ashby, Mater. Sci. Technol. 8 (1992) 594–601.
[2] U.P. Singh, H.D. Merchant, Metall. Trans. 4 (1973) 2621.
[3] H.D. Merchant, G.S. Murty, S.N. Bahadur, L.T. Dwivedi, Y. Mehrotra, J. Mater. Sci. 8 (1973) 437–442.
[4] O.D. Sherby, P.E. Armstrong, Metall. Mater. Trans. B 2 (1971) 3479–3484.
[5] R.M. Hooper, C.A. Brookes, J. Mater. Sci. 19 (1984) 4057–4060.
[6] G. Cseh, N.Q. Chinh, P. Tasnadi, A. Juhasz, J. Mater. Sci. 32 (1997) 5107–5111.
[7] G. Cseh, N.Q. Chinh, A. Juhasz, J. Mater. Sci. 17 (1998) 1207–1209.
[8] M. Fujiwara, M. Otsuka, J. Mater. Sci. Eng. A 319–321 (2001) 929–933.
[9] U.K. Viswanathan, T.R.G. Kutty, R. Keswani, C. Ganguly, J. Mater. Sci. 31 (1996) 2705–2709.
[10] B.N. Lucas, W.C. Oliver, Metall. Mater. Trans. A 30A (1999) 601.
[11] J.C.M. Li, S.N. Chu, J. Mater. Sci. 12 (1977) 2200–2208.
[12] S.N.G. Chu, J.C.M. Li, J. Mater. Sci. Eng. 39 (1979) 1–10.
[13] S.H. Wang, J. Mar. Sci. Technol. 2 (1994) 17–24.
[14] H.Y. Yu, J.C.M. Li, J. Mater. Sci. 12 (1977) 2214–2222.
[15] D. Chiang, J.C.M. Li, J. Mater. Res. 9 (1994) 903–908.
[16] E.C. Yu, J.C.M. Li, Philos. Mag. 36 (1977) 811–825.
[17] D. Dorner, K. Roller, B. Skrotzki, B. Stockhert, G. Eggeler, Mater. Sci. Eng. A 357 (2003) 346–354.
[18] L. Peng, F. Yang, J.-F. Nie, J.C.M. Li, Mater. Sci. Eng. A 410–411 (2005) 42–47.

[19] P.S. Gondavarti, K. Linga Murty, J. Mater. Sci. Lett. 6 (1987) 456–458.
[20] G. Nayyeri, R. Mahmudi, Mater. Sci. Eng. A 527 (2010) 2087–2098.
[21] T.H. Hyde, K.A. Yehia, A.A. Becker, Mater. High Temp. 13 (1995) 133–138.
[22] M.D. Mathew, K. Laha, V. Ganesan, Mater. Sci. Eng. A 535 (2012) 76–83.
[23] M.D. Mathew, Trans. Indian Inst. Met. 63 (2010) 151–158.
[24] M.D. Mathew, V.S. Srinivasan, in: U. Kamachi Mudali, B. Raj (Eds.), Mechanical Behavior of Nitrogen-bearing steels in Monograph on High Nitrogen Steels and Stainless Steels, Narosa Publications, New Delhi, 2004, pp. 182–204.
[25] V. Ganesan, M.D. Mathew, K.B. Sankara Rao, Mater. Sci. Technol. 25 (2009) 614–618.
[26] J.W. Simmons, Mater. Sci. Eng. A 207 (1996) 159–169.